Sustainable Food Technology

Accepted Manuscript

Sustainable
Food Technology

ROYAL SOCIETY
OF CHEMISTRY

ROYAL SOCIETY
OF CHEMISTRY

Sustainability Spotlight Statement

Millets are climate-resilient, nutrient-dense grains critical for global food and nutrition security, yet their wider use is limited by processing challenges. Conventional processing often depletes nutrients and demands high energy, contradicting sustainable practices. This study demonstrates the application of non-equilibrium cold plasma (NECP), a non-thermal, chemical-free, and energy-efficient technology, to enhance the functional and thermal properties of pearl and sorghum millet flours without compromising quality. By improving flour performance for gluten-free and functional food applications, the work promotes sustainable food diversification and supports resilient food systems. This aligns with UN Sustainable Development Goals (SDG 2: Zero Hunger, SDG 3: Good Health and Well-being, and SDG 12: Responsible Consumption and Production).

1   **Non-Equilibrium Cold Plasma as a Sustainable Approach to Improve**

2   **Functional and Thermal Properties of Pearl and Sorghum Millet Flours**

3   Ritesh Mishra[1], Sushma Jangra[2], Abhijit Mishra[2], Shikha Pandey[2], Meenu Chhabra[3,1], and

4   Ram Prakash[2,1]

5   [1]Inter-Disciplinary Research Division-Smart Healthcare, Indian Institute of Technology,

6   Jodhpur, Rajasthan, India

7   [2]Department of Physics, Indian Institute of Technology, Jodhpur, Rajasthan, India

8   [3]Department of Bioscience and Bioengineering, Indian Institute of Technology, Jodhpur,

9   Rajasthan, India

10 *Corresponding Author e-mail: ramprakash@iitj.ac.in

11

12 **Abstract**

13 This study investigates the effects of non-equilibrium cold plasma (NECP) treatment using air

14 plasma and transient exposure methods on the functional, structural, and thermal properties of

15 pearl and sorghum millet flours. Pearl and sorghum millet flour were treated at two different

16 exposure times for 5 min and 10 min, and functional properties such as Water and oil holding

17 capacity, water binding capacity, color, and dispersibility of the control and plasma-treated

18 flour were studied. There was no significant difference in the color intensity and the whitening

19 index (WI) with the treatment. However, the 10-minute treatment resulted in an increase in

20 water absorption capacity (1.55–1.81 g/g), oil absorption capacity (1.21-1.4 g/g), and water

21 binding capacity (2.25-2.37 g/g) in pearl millet flour. Similarly, sorghum millet flour water

22 absorption capacity (1.43 to 1.74 g/g), oil absorption capacity (1.08 to 1.27 g/g), and water

23 binding capacity (2.07-2.26 g/g) increase with 10 min NECP treatment. In addition, Fourier

24 transform infrared spectrometry analysis detected shifts in functional groups, X-ray diffraction

25 analysis indicated changes in crystallinity, and Differential crystallography showed a reduction

26 in gelatinization enthalpy. Overall, plasma treatment can be explored for the development of a

27 process to enhance the functionality of millet flour for applications in food systems.

28 **Keywords:** Non-equilibrium cold plasma, pearl millet flour, sorghum millet flour, functional

29 properties, thermal properties

30

1.   Introduction

Millets, a type of grass, are distinguished by their compact, slender stems and minuscule seeds, both of which exhibit remarkable resistance to extended periods of drought. Millets are considered to be among the earliest cereal grains farmed for the sake of subsistence (1). Millets are widely known as "smart food." Millets are a highly nutritious food, rich in iron, folate, calcium, zinc, magnesium, phosphorus, copper, vitamins, fiber, and antioxidants. In addition, besides being essential for the proper development and maturation of children, they have been shown to reduce the risk of heart disease and diabetes in adults. In addition, Millet is a suitable choice for individuals with coeliac disease or gluten-related illnesses such as wheat allergy and non-celiac gluten sensitivity, which can have significant health consequences when even little amounts of gluten are consumed (2). There has been a rise in demand for gluten-free products among individuals seeking to adhere to a nutritious diet. To achieve this, it is imperative to enhance and broaden the food business by advancing the development of ingredients and formulations, as well as increasing the production of functional foods (3). Sorghum (Sorghum bicolor) and Pearl millet (Pennisetum glaucum) are two significant millet varieties that are renowned for their nutritional advantages and are frequently utilized for producing gluten-free flour. These grains are currently receiving more attention from food scientists, nutritionists, and policymakers because of their socio-economic consequences (4). To globally promote and popularize these millets, it is essential to create advanced processing techniques that specifically aim to increase the functional and structural properties of millet flour. However, the emphasis on the processing and enhancement of millet flours is currently limited due to the lack of awareness regarding their nutritional and health advantages among the population. While various research has employed boiling, microwave treatment, cooking, and autoclaving for processing (5). These technologies adversely affect the nutritional properties of the flour. This has urged the need to investigate the applicability of non-thermal technologies like cold plasma.

Non-equilibrium Cold plasma (NECP) treatment is a highly adaptable method that can be used in various applications in the food industry. It can be used to modify the structure of macromolecules like starch, protein, and cellulose, promote seed germination, eliminate microbes, and extract bioactive chemicals (6). The NECP treatment is an acknowledged non-thermal technology, classified as the fourth state of matter. It is a partially ionized gas that consists of free radicals, photons, ozone, energetic ions, and free electrons in either the ground

63 or excited state (7–9). The studies reported that the treatment of cold plasma had a significant

64 impact on the functional, rheological, and thermal properties of various types of flour,

65 including wheat flour, quinoa flour, jackfruit seed flour, little millet flour, and bamboo rice

66 flour (10–15). However, there has been little research conducted on the effects of various

67 treatment conditions on the nutritional and antinutritional components, as well as the functional

68 and thermal properties of millet flours. R et al. (2021) (16) exposed the pearl millet to cold

69 plasma technology at 180 V with a 0.01 m³/h airflow rate. The study concluded that the phytic

70 acid content was reduced by 60.66% and 39.27% when the treatment was operated on for 1

71 and 2 h, respectively. Jaddu, Pradhan et al. (2022) (12) reported that the crystallinity of the

72 little millet flour reduces due to the depolymerization of starch during the cold plasma

73 treatment. They also showed that the treatment increased the water absorption capacity (WAC),

74 oil absorption capacity (OAC), swelling capacity, and solubility index of the flour. The impacts

75 of ultra-high pressure coupled with cold plasma treatment on physical, chemical, and digestive

76 qualities are investigated in another research on proso millet starch (17).

77 Previous studies on flour properties utilized either a pin-type or a multipin cold plasma setup

78 (18–23). This device has the capability to generate plasma distributions that are not uniform,

79 resulting in uneven treatment over the surface area. The treatment region for pin-type devices

80 is often confined to the immediate vicinity of the pin electrodes. When dealing with big regions

81 or volumes, it is necessary to either make many passes or use an array of pins, which makes

82 the operation more complex. Attaining a fully homogeneous plasma treatment might be

83 challenging, even with the utilization of several pins. Inconsistent treatment effects can result

84 from variations in plasma intensity among pins. Moreover, the intense concentration of energy

85 around the pin electrodes can lead to localized surface harm or deterioration, particularly for

86 delicate materials. In addition, Pin electrodes are prone to experiencing wear and erosion as

87 time passes, which requires frequent maintenance and replacement. This leads to higher

88 operational expenses and periods of inactivity. In contrast to earlier investigations, air plasma

89 is used in our experiment, and the flours can be treated with transient exposure to non-

90 equilibrium cold plasma. The momentary exposure strategy enhances commercial feasibility,

91 as it can be readily integrated into existing flour processing lines without requiring substantial

92 redesign or major infrastructural modifications, making the approach scalable, energy-

93 efficient, and industry-friendly (24). The transient plasma exposure ensures sufficient

94 interaction between plasma-generated reactive oxygen and nitrogen species (RONS) and flour

95 constituents while minimizing excessive energy input and thermal stress. This short-duration,

96   non-equilibrium treatment helps preserve the intrinsic nutritional and functional attributes of

97   pearl millet flour, while still inducing desirable modifications such as improved hydration

98   behavior, surface activation, and microbial reduction.

99   During the plasma discharge, the presence of electrons, ions, and excited species leads to their

100   interaction with the surrounding air, resulting in the formation of different reactive oxygen-

101   nitrogen species (RONS)[25]. The major species believed to be responsible for these reactive

102   oxygen and nitrogen species (RONS) include atomic oxygen (O), ozone (O_3), hydroxyl radicals

103   (OH), nitric oxide (NO), and hydrogen peroxide (H_2O_2) [26,27]. Therefore, this study aimed

104   to examine the effects of NECP treatment on several aspects, including nutritional factors,

105   functional and thermal characteristics, changes in pearl millet flour (PMF), and sorghum millet

106   flour (SMF). Furthermore, the effects of NECP treatment on several characteristics of PMF

107   and SMF were examined in further detail using principal component analysis to determine the

108   optimal operating parameters. In addition, the use of NECP treatment might be employed to

109   create functional foods and may have motivated the research community to create more

110   sustainable, environmentally friendly, and energy-efficient technologies for millet processing.

111   By improving flour performance for gluten-free and functional food applications, the work

112   promotes sustainable food diversification and supports resilient food systems. This aligns with

113   UN Sustainable Development Goals (SDG 2: Zero Hunger, SDG 3: Good Health and Well-

114   being, and SDG 12: Responsible Consumption and Production).

115   2. Materials and Methods

116   The pearl millet flour (FMF) and sorghum millet flour (SMF) were obtained from the local

117   market in Jodhpur, Rajasthan, India. The experiments were carried out at ambient temperature

118   in the Cold Plasma Laboratory, located in the Department of Physics at IIT Jodhpur. The

119   analysis was conducted at the Environmental Biotech Lab, located in the Department of

120   Bioscience and Bioengineering at IIT Jodhpur. The functional characteristics, such as Water

121   Holding Capacity (WHC), Oil Holding Capacity (OHC), Water binding capacity (WBC),

122   Dispersibility, color, foaming capacity (FC), and emulsifying capacity (EC), were evaluated

123   for 5- and 10-minute NECP treatment time using the methodologies described elsewhere

124   [20,28]. Bioactive compounds like total phenolic content (TPC) and total flavonoid content

125   (TFC) were measured according to Mishra et al. (2024) [29] with slight modification. The

126   Fourier transform infrared spectra of millet flours treated with cold plasma were recorded using

127   FTIR spectroscopy (Bruker, Alpha E FTIR, Germany) with attenuated total reflectance (ATR).

128   The Perkin Elmer DSC-4000, a differential scanning calorimeter, was employed to determine

129   the peak temperatures of finger millet flour treated with plasma.

130   **2.1 Experimental setup**

131   The experimental setup implemented for the treatment of the millet flour as shown in Fig. 1

132   The stator and rotator device are powered by the aforementioned variable bipolar pulsed power

133   supply (Grow controls, GC253HVPS), which is coupled with a high voltage probe (1000x,

134   P6015A, Tektronix) and current monitor (Pearson 110) for monitoring the applied voltage (V)

135   and discharge current (I) waveforms which can be directly visualised by a four-channel digital

136   oscilloscope (MDO3014, 100 MHz, Tektronix). The system consists of a Teflon sleeve rotator

137   connected to an aluminium shaft, which is secured to a holder using a nylon gear wheel to

138   maintain a 1.0 mm distance. The stator is composed of an aluminium shaft of the same size,

139   supplied with an identical gear wheel on two side stands. A 1.5 mm thick hollow dielectric

140   material (dielectric constant: 2.1) was placed over a solid aluminium rod measuring 110 mm

141   in length and 15 mm in diameter to cover the stator electrode that was utilized as the cathode.

142   Another aluminium hollow electrode having the same length and diameter as the first, but

143   inside the hollow electrode was used as an anode. The same dielectric material was filled

144   similar to the solid aluminium rod. Plasma discharge was produced at atmospheric pressure,

145   and ambient air was used as the gas carrier between the two electrodes. The high voltage (H.V.)

146   probe was linked to the digital oscilloscope, while a wire connector was used to connect the

147   H.V. probe between the high voltage electrode and the power supply. The high-voltage probe

148   was also appropriately grounded. The wire was attached to the grounded electrode of the device

149   and then passed through a current monitor (CT). The output of the CT was then linked to the

150   digital oscilloscope. The study employed Optical Emission Spectroscopy (OES) (Andor

151   Shamrock SR-500i-B1) to investigate the species produced in an air plasma (Fig. 2). Optical

152   emission spectroscopy (OES) was used to examine the gas phase of cold plasma**.** The spectrum

153   of dielectric barrier discharge under atmospheric pressure plasma was shown in Fig. 2 from

154   200 to 400 nm and 500 to 900 nm. The spectra from 200 to 400 nm were composed of nitrogen

155   and nitric oxide. NO is produced within the wavelength of 236 to 283 nm. The spectra were

156   characterised by prominent peaks associated with N_2 second positive system (SPS, C-B)

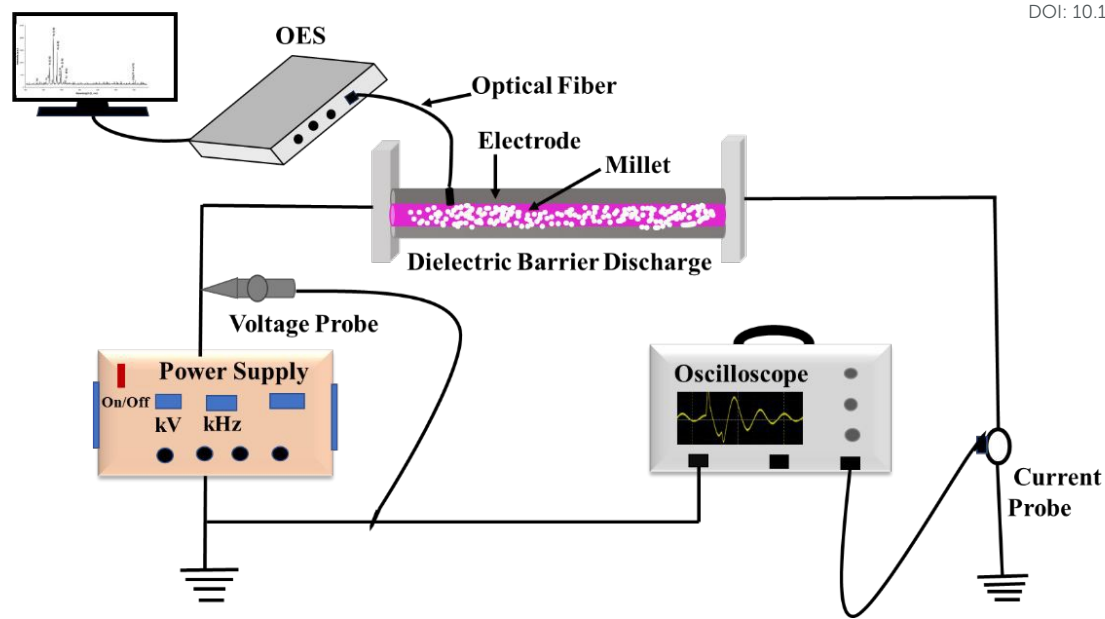157   emissions at wavelengths of 315.7, 337.3, 353.6, 357.7, 375.5, 380.5 nm (30).

158

159

160   Fig. 1 A schematic illustration of the experimental setup for DBD discharge plasma treatment

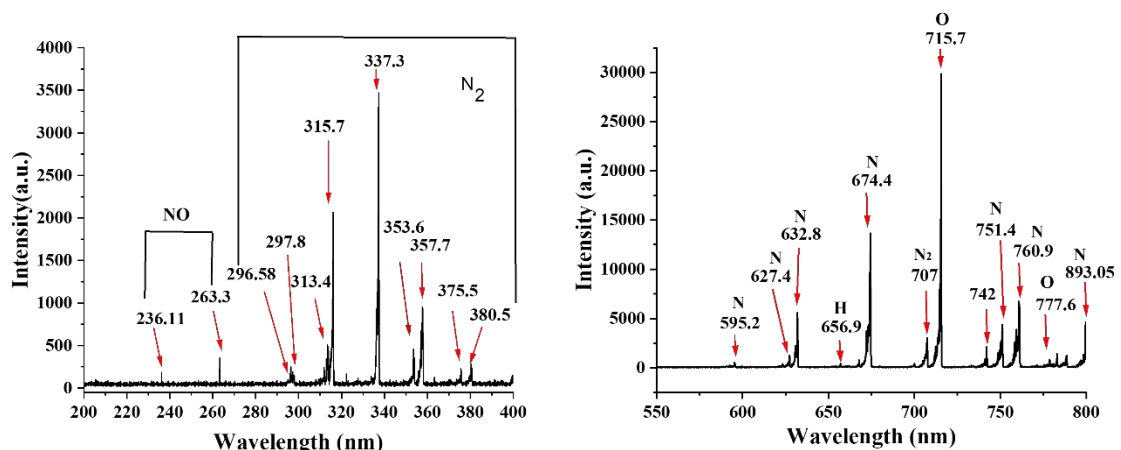161   of millet flour.

162

163   Fig. 2 Optical emission spectrum of DBD Plasma at (a) 200 to 400 nm and (b) 550 to 800 nm

164

165   The preliminary experiments were performed to investigate the treatment efficiency at various

166   voltage levels. It was observed that the plasma discharge initiated at a breakdown voltage of 6

167   kV, stabilized at 7 kV, and remained stable until 9 kV. Due to the impact on the high voltage

168   electrode, it is not suggested to perform prolonged plasma treatments. Moreover, exceeding a

169   specific duration of treatment fails to significantly improve the desired outcomes. Prolonged

170   treatment durations can result in physical harm to the material being treated, including surface

171   erosion, alterations in texture, or compromised structural integrity. Furthermore, when exposed

172   to high voltage for an extended period, the substantial energy released during plasma discharge

173   has the ability to deteriorate nutritional components present in millet flours, including vitamins,

174   amino acids, and antioxidants. Attaining consistent plasma treatment for every individual flour

175   particle can be a challenge. Non-uniform treatment can lead to variations in the quality and

176   functionality of food products. Therefore, we fine-tune our device to achieve the most effective

177   treatment duration. This includes treatment times of up to 20 minutes at 7 KV and up to 10

178   minutes at 9 KV. In our previous work, we used NECP treatment on finger millet flour at 7 KV

179   and found that higher voltage will increase the crystallinity of the flour, thereby increasing its

180   functionality (15). Consequently, the parameters selected for the treatment of PMF and SMF

181   were established as 9 KV for a duration of 5-10 minutes.

182   **2.2 Functional Properties**

183   The functional properties, including Water absorption capacity (WAC), Oil absorption capacity

184   (OAC), Water binding capacity (WBC), Dispersibility, foaming capacity (FC), and

185   emulsifying capacity (EC), were assessed for control as well as NECP-treated pearl millet and

186   sorghum millet flours using the specified methodology (20,28).

187   To obtain water binding capacity (WBC), 1.0 g of millet flour samples was combined with 10

188   ml of deionized water and subjected to centrifugation at 2000 g for 10 min. WBC was

189   calculated using the expression given by Quinton (2002) (31). WBC was determined as the

190   ratio of grams of water retained to grams of solid. The WAC and OAC were determined by

191   employing the methods with minor alterations outlined by Chaple et al. (2020) (28). The WAC

192   and OAC were determined using Equation (1).

193

194   **WAC and OAC (g/g)** $= \dfrac{Sample\ weight\ after\ centrifugation - Initial\ sample\ weight}{Initial\ sample\ weight}$ **(1)**

195

196   **Emulsifying and Foaming Capacity**

197   To determine the emulsifying capacity (EC), a solution containing 0.5 grams of millet flour, 5

198   ml of distilled water, and 5 ml of soybean oil was made in a centrifuge tube. The mixture was

199   mixed using a vortex and then centrifuged at a force of 340 g for 10 minutes. The resulting

200   suspension was carefully transferred to a graduated cylinder, and the total volume as well as

201   the volume of the emulsion layer were precisely measured.

202   The EC (%) was calculated using Equation (2) as specified by Kheto et al. (2022) (32);

203    $$\textbf{EC (\%)} = \frac{\textbf{\textit{emulsion volume (mL)}}}{\textbf{\textit{total volume (mL)}}} \textbf{ X 100} \quad \textbf{(2)}$$

204

205   To measure foaming capacity (FC), 1 gram of millet flour with 50 ml of distilled water was

206   mixed in a beaker. The solution was aggressively stirred for 5 minutes and immediately put

207   into a measuring cylinder. The volume of foam generated was recorded, and FC (%) was

208   determined using Equation (3):

209    $$\textbf{FC (\%)} = \frac{\textbf{\textit{volume after shaking (mL)} − \textit{inital volume of suspension}}}{\textbf{\textit{inital volume of suspension (mL)}}} \textbf{ X 100} \quad \textbf{(3)}$$

210

211   **Dispersibility**

212   A measured quantity of 10 g of flour was mixed with 100 ml of deionized water, and placed in

213   a 100 ml measuring cylinder. The components are blended and left undisturbed for a duration

214   of 3 hours. The dispersibility of flour was determined by subtracting the volume of settled

215   particles from 100 (33).

216   **2.3 Color**

217   The color values L*, a*, b*, ΔE of PMF and SMF (control and NECP treated) were observed

218   by color reader CR6 (3nh). The L*, a*, b*, ΔE, hue angle, whitening index (WI), yellow index

219   (YI), and browning index (BI) values of PMF and SMF (both control and NECP treated) were

220   determined using equations 4-8 given elsewhere (34,35).

221   Hue angle **(H)** = $\textbf{tan}^{-1} \dfrac{\textbf{\textit{b}}}{\textbf{\textit{a}}}$ $\qquad\qquad\qquad$ **(4)**

222   Total color difference **(ΔE)** = $\sqrt{\mathbf{\Delta L^{*2} + \Delta a^{*2} + \Delta b^{*2}}}$ $\qquad$ **(5)**

223   Whitening index **(WI)** = $\sqrt{\mathbf{(100 - L^*)^2 + a^{*2} + b^{*2}}}$ $\qquad$ **(6)**

224   Yellow index **(YI)** = $\dfrac{\mathbf{142.86 b^*}}{\mathbf{L^*}}$ $\qquad\qquad$ **(7)**

225   Browning index **(BI)** = $\dfrac{\mathbf{[100 \times (X - 0.31)]}}{\mathbf{0.172}}$ $\qquad\qquad$ **(8)**

226   Where, X = $(a^* + 1.75 \times L^*) / (5.645 \times L^* + a^* - 3.012 \times b^*)$

227   **2.4 Bioactive compounds**

228   The sample extracts were prepared according to the procedure outlined by Kheto et al. (2022)

229   (32). Then the prepared sample extract was used to estimate the total phenol content (TPC; g

230   of GAE in 100 g of dm), and total flavonoid content (TFC; g of QE in 100 g of dm).

231   **2.5 Fourier transform infrared spectrometry**

232   The FTIR spectra of the PMF and SMF samples were acquired to assess the functional group

233   variations using a FTIR spectrophotometer (Bruker, Alpha E FTIR, Germany) with attenuated

234   total reflectance (ATR). Samples were gently placed on a ZnSe crystal and scanned at 64 scans

235   per sample to obtain % transmittance at specific wavenumbers ranging from 4000 to 400 cm^1

236   (32)

237   **2.6 Thermal properties**

238   The thermal properties of PMF and SMF samples were determined by a differential scanning

239   calorimeter (Perkin Elmer DSC-4000), to determine the peak temperatures of millet flours

240   treated with plasma in the range of 20 to 220 °C at 10°C per min, as reported by Kheto et al.

241   (2022)(32).

242   **2.7 Field emission Scanning electron microscopy (FESEM) analysis**

243   The morphology of the PMF and SMF samples was examined using a field emission scanning

244   electron microscopy (Thermo Fisher Apreo-2 at 5 kV acceleration voltage). Before imaging,

245   both control and NECP-treated samples were sputtered with gold using a DC sputter. FESEM

246   imaging was then performed to visualize the microstructural variations (24).

247   **2.8 X-ray diffractogram analysis**

248   The PMF and SMF samples were analysed using an X-ray diffractometer (Bruker AXS D8

249   Advance, Germany) to obtain their X-ray diffractograms (XRD). The samples were subjected

250   to an X-ray beam with an intensity of 15 mA and a voltage of 30 kV to investigate the intensity

251   pattern of crystallinity within the 2θ range of 4–45, using a steep angle of 0.02 and a scan rate

252   of 5/min (32).

253   **2.9 Antinutritional factors**

254   To evaluate the influence of NECP on antinutritional components in PMF and SMF, both

255   tannins and phytic acid were quantified in untreated and plasma-treated samples. Tannin

256   analysis was carried out following the procedure described by Yadav et al. (2021)(36). Briefly,

257   1 g of flour was extracted using 10 mL of acidified methanol (HCl: methanol = 1:100), and

258　centrifuged at 6000 rpm for 20 minutes. Then, 1mL of extract was mixed with 5 mL of vanillin

259　reagent and allowed to react for 20 minutes. The absorbance of the developed color was then

260　recorded at 500 nm using a UV-visible spectrophotometer (UV-1800, Shimadzu, Japan).

261　Phytic acid was estimated by the method given by Yadav et al. (2021)(36). Briefly, 0.1 g of the

262　sample was extracted using 10 mL of 0.2 mol/L hydrochloric acid and allowed to stand for 1

263　hour. The mixture was then centrifuged at 5000 rpm for 15 minutes, and later 0.5 mL of the

264　clear supernatant was carefully transferred into a glass-stoppered test tube. An iron (III) reagent

265　was prepared by dissolving 0.2 g of ammonium iron (III) sulfate dodecahydrate in 100 mL of

266　2 mol/L HCl and diluting to 1 L with distilled water. Accordingly, 1 mL of this reagent was

267　added to the sample and the sample was heated for 30 minutes and subsequently cooled in an

268　ice water bath to 25 ˚C. Then 2 mL of bipyridine solution (10 g of 2,2′-bipyridine and 10 mL

269　thioglycolic acid in 1 L of distilled water) was added to the test tube. After 1 minute, absorbance

270　was recorded at 519 nm using a UV-Vis spectrophotometer (UV-1800, Shimadzu, Japan).

271　**2.10 Statistical analysis**

272　The studies were conducted in triplicate, and the results were provided as the mean standard

273　deviation. The statistical significance was assessed using the Duncan test. In addition, principal

274　component analysis (PCA) was conducted using Origin pro 2023 software from OriginLab,

275　USA, to determine the optimal condition.

276　**3.　Results and Discussion**

277　**3.1.Plasma characteristics**

278　A typical V-I characteristic of the above-described DBD source is shown in Fig. 3. The electric

279　power dissipated into the plasma is calculated from waveforms of applied voltage (Ut) and the

280　discharge current (i$_t$), using the following relationship (37) .

281
$$P_{avg} = \frac{1}{T}\int_0^t P_t \, dt$$

282　Where T is the period of oscillation, P (t) is the instantaneous power calculated by

283　multiplying the instantaneous voltage V(t) and current I(t).

284　The electron density can be approximated from the V–I curve using the following

285　relationship (11):

286
$$n_e = \frac{J}{e\mu_e E} = \frac{I_{rms}}{Ae\mu_e E}$$

287   where J is the current density, A is the cross-sectional area of the powered electrode, Irms

288   is the root mean square current, E is the electric field between the electrodes, e is the

289   electronic charge, and μe is the electron mobility, i.e., 552 cm2/V.s in the case of nitrogen.

290   The operational condition results in approximately an average power consumption of 10 W

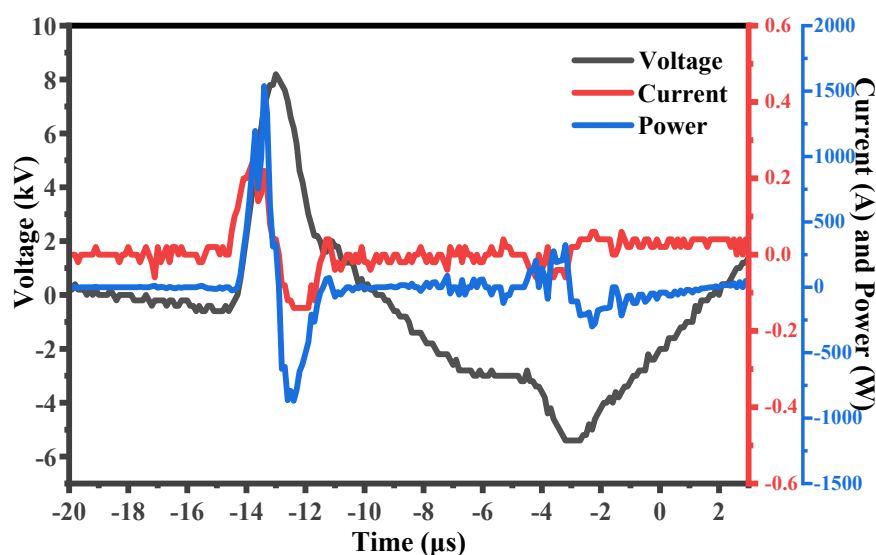291   and an electron density of 4.19×10^9 particles/cm^3

292

293   Fig. 3 Typical V–I characteristics for DBD 9 kV/20 kHz.

294   **3.2 Effect of NECP on functional characteristics of millet flour**

295   The functional characteristics of PMF and SMF for control (PMFC and SMFC) and NECP-

296   treated samples for 5 minutes (PMF5 and SMF5) and 10 minutes (PMF10 and SMF10) are

297   presented in Table 1. The functional characteristics of all treated samples were substantially

298   enhanced through NECP-treatment, which was maximum for the 10-minute treated samples.

299   The oil and water absorption capacity of plasma-treated PMF and SMF showed a positive

300   correlation with increasing treatment time. The untreated PMF and SMF exhibited an oil

301   absorption capacity of 1.21± 0.041 g/g and 1.08±0.02 g/g, and a water absorption capacity of

302   1.55±0.083 g/g and 1.43±0.042 g/g, respectively. The OAC of PMF10 and SMF10 had a

303   maximum value of 1.4±0.034 g/g and 1.27±0.015 g/g, which were significantly (P<0.05) higher

304   than the untreated samples (PMFC and SMFC). Similarly, the WAC of PMF10 and SMF10

305   had significantly (P<0.05) higher values, 1.81±0.094 and 1.74±0.08, compared to the untreated

306   samples. The increase in OAC and WAC is attributed to the existence of plasma-generated

307   species, such as ions and radicals. These species improve the hydrophilic characteristics of

308   flour, with the degree of starch molecule degradation after NECP treatment contributing to this

309   enhancement (38). Furthermore, the degradation of starch is mostly attributed to the influence

310 of high-energy plasma species and the partial oxidation of starch, particularly by ozone,

311 resulting in the formation of carboxylic starch. In addition, it is possible that the sample treated

312 with NECP had a higher concentration of hydrophilic sites, including proteins, carbohydrates,

313 and certain residues of polar amino acids. The NECP treatment causes the depolymerization of

314 starch particles, increasing amylose content. This increase in amylose content leads to an

315 increase in crystallinity, which is also associated with increased water absorption capacity. The

316 FTIR results support these findings. Additionally, the NECP treatment causes the formation of

317 fissures and dents, which provide more sites for lyophilic groups. This ultimately leads to an

318 increase in the oil absorption capacity (OAC) of the flour. Similar findings were reported

319 elsewhere (20,39). However, Chaple et al. (2020) (28) noticed that there were no notable

320 changes in the OAC of wheat flour when exposed to 80kV plasma for durations ranging from

321 5 to 30 minutes. They observed that the quantities of protein and nonpolar amino acids

322 exhibited fluctuations, although these variations were deemed insignificant. Increased WAC

323 and OAC levels have the intriguing impact of enhancing the volume and texture of baked food

324 products, this attribute makes them well-suited for various baking purposes (40).

325 The water binding capacity (WBC) of NECP-treated flour was enhanced by the plasma

326 treatment, as shown in Table 1. The WBC of the control (PMFC and SMFC) samples were

327 2.25 ± 0.059 and 2.01 ± 0.007, respectively, which had a significantly higher (P<0.05) value for

328 the 10-minute treated samples. The WBC of PMF10 and SMF10 were determined as

329 2.37 ± 0.021 and 2.26 ± 0.055, while for PMF5 and SMF5, the value of WBC was recorded as

330 2.34 ± 0.016 and 2.11 ± 0.003, respectively. Similarly, Chaple et al. (2020) (28) reported that

331 plasma treatment resulted in an enhancement in the water binding capacity (WBC) of flour.

332 The flour's hydration characteristics are enhanced by plasma treatment, indicating that the

333 higher surface area resulting from the initial plasma treatment influences the hydration qualities

334 of the flours. This information can be considered in order to meet specific functional needs

335 Furthermore, as compared to the control, the NECP-treated samples showed significantly

336 higher (P<0.05) values for EC and FC. The control PMF and SMF exhibit an EC value of

337 $61.86\pm0.51\%$ and $61.29\pm0.023\%$ (Table 1), respectively. Following a 10-minute plasma

338 treatment, the EC value exhibited a rise to $64.12\pm0.635\%$ and $63.21\pm0.084\%$. The increase can

339 be ascribed to the improved disorganized arrangement, which allows the proteins to engage

340 with both water and oil. Consequently, the ability of the emulsion to hold and disperse

341 substances is enhanced, and the creation of air bubbles is increased (41). The FC value of the

342 treated PMF10 and SMF10 significantly increased (p<0.05) to 13.18±0.282 % and

343 12.19±0.337 % respectively, compared to the control PMFC and SMFC with an FC value of

344 11.57±0.492 % and 10.44±0.22 %, respectively. Sarkar et al. (2023) (21) observed that the

345 plasma treatment of the pearl millet surface leads to the exposure of hydrophobic groups, which

346 in turn attract oil droplets and enhance the stability of the emulsions formed. In addition, the

347 plasma treatment may have raised the surface elasticity; this higher elasticity allows the protein

348 to stretch and deform around the oil droplets and air bubbles, resulting in an enhanced FC (42).

349 The NECP treatment did not affect the dispersibility of the PMF and SMF samples. Similar

350 findings were reported elsewhere (12).

3.3 Bioactive compounds (total phenol content and total flavonoid content)

352 The NECP treatment did not have a significant impact on the values of total phenolic content

353 and total flavonoid content (TPC) and (TFC), as shown in Table 1. The TPC of the PMFC was

354 determined to be 2.39±0.08 (mg GAE/100 g dm). The TPC decreased as the treatment duration

355 increased from 5 to 10 minutes. The TFC of the PMFC sample was 2.17±0.092 (mg QE/100 g

356 dm), which decreased with the NECP treatment. Similarly, the TFC of SMFC was measured

357 to be 2.22±0.04, which reduces to 2.14±0.03 and 2.09±0.023 (p <0.05) for SMF5 and SMF10,

358 respectively. The TFC has also decreased after NECP treatment, which was recorded as

359 1.65±0.031 for SMF5 and 1.60±0.023 for SMF10, whereas the untreated sample (SMFC) had

360 a TFC value of 1.73±0.05. The minor decline in TPC (Total Phenolic Content) and TFC (Total

361 Flavonoid Content) indicates that plasma discharge generates high-energy electrons that,

362 through direct interaction with phenolic compounds, induce the dissociation of oxygen

363 molecules and subsequently lead to deterioration (10,12). Furthermore, a decrease in phenolic

364 compounds can potentially contribute to the generation of ozone and other reactive species

365 through dissociation, a process in which individual oxygen atoms unite with oxygen molecules

366 to produce ozone. Conversely, aliphatic molecules, such as hydroxylated and quinone

367 compounds, are produced through the reaction of molecular ozone with the aromatic rings of

368 phenolics, leading to the breakdown and deterioration of phenolic compounds (21). Additional

369 investigation is required to comprehend the interaction between phytochemicals and reactive

370 species. Overall, the recent findings corroborated the results of the previous study by Sarkar et

371 al. (2023) and Almeida et al. (2015) (21,43), which revealed a decrease in phytochemicals

372 following CP treatment.

373

374   Table 1. Effect of NECP on functional characteristics of finger millet flour

	PMFC	PMF5	PMF10	SMFC	SMF5	SMF10
Water Absorption Capacity (WAC) (g/g)	1.55±0.083[b]	1.68±0.04[ab]	1.81±0.094[a]	1.43±0.04[b]2	1.52±0.1[b]	1.74±0.08[a]
Oil Absorption Capacity (OAC) (g/g)	1.21±0.041[a]	1.28±0.03[b]	1.4±0.034[c]	1.08±0.02[c]	1.15±0.03[b]	1.27±0.015[a]
Water Binding Capacity (WBC) (g/g)	2.25±0.059[b]	2.34±0.016[a]	2.37±0.021[a]	2.01±0.007[c]	2.11±0.003[b]	2.26±0.055[a]
Total Phenol Content (TPC) (mg GAE/100 g dm)	2.39±0.08[NS]	2.34±0.072[NS]	2.25±0.035[NS]	2.22±0.04[b]	2.14±0.03[ab]	2.09±0.023[a]
Total Flavonoid Content (TFC) (mg QE/100 g dm)	2.17±0.092[NS]	2.16±0.1[NS]	2.04±0.035[NS]	1.73±0.05[b]	1.65±0.031[b]	1.60±0.023[a]
Emulsifying Capacity (EC) %	61.86±0.51[b]	62.38±0.21[b]	64.12±0.635[a]	61.29±0.023[c]	62.33±0.087[b]	63.21±0.084[a]
Foaming Capacity (FC) %	11.57±0.492[b]	12.39±0.385[ab]	13.18±0.282[a]	10.44±0.22[c]	11.11±0.217[b]	12.19±0.337[a]
Dispersibility %	79.02±0.921[b]	76.81±0.737[ab]	74.13±1.11[a]	77.78±0.683[c]	74.29±0.858[b]	71.46±0.51[a]

375   Means with different superscripts in the same row represent significant ($p < 0.05$) differences

376   with each other.

377

378   **3.4 Effect of NECP on Color**

379   The color attributes of cold plasma-treated and untreated PMF and SMF were assessed and

380   reported in Table 2. The results were derived using the CIELAB (L*, a*, b*) color space. L*

381   represents lightness, while a* and b* represent red-greenness and blue-yellowness, respectively

382   (44). The L* value of PMF samples varied between 46.01±0.02 to 46.325±0.175. The flour

383   experienced no reduction in its L* value following the NECP treatment. This shows that NECP

384   treatment has no effect on L* values, indicating similar hue for the treated and untreated PMF

385   samples. The values a* and b* of all the samples range from 0.635±0.005 to 0.625±0.035 and

14

386 from 0.855±0.005 to 0.825±0.015, respectively. The L* value of the SMF samples ranged from

387 47.525±0.015 to 47.395±0.015. The NECP treatment did not cause any decrease in the L* value

388 of the flour. The results demonstrate that NECP treatment does not impact the L* values,

389 indicating that the hue of the treated and untreated SMF samples is similar. The values of a*

390 and b* for all the samples vary between 0.855±0.005 and 0.88±0.01, and between 1.685±0.045

391 and 1.495±0.015, respectively. The lack of significant shifts in color values implies that non-

392 equilibrium cold plasma does not induce any changes in the product's color. The whitening

393 index (WI), yellow index (YI), and hue angle (h*) of the plasma-treated pearl millet flour

394 remains unchanged with the different treatment times. However, there was only a minor overall

395 change in color observed, and this shift can be attributed to the surface structure of the particles,

396 which is significantly affected by plasma and is evident in the optical characteristics of flour.

397 Due to the surface etching caused by plasma treatment, it is expected that there would be

398 changes in the color values of the treated product (13).

399 Table 2. Effect of NECP on Color of pearl and sorghum millet flour

Color Index	PMFC	PMF5	PMF10	SMFC	SMF5	SMF10
L*	46.01±0.02[NS]	46.035±0.015 [NS]	46.325±0.175 [NS]	47.525±0.015 [a]	47.30±0.01[b]	47.395±0.015[b]
a*	0.635±0.005 [NS]	0.655±0.01 [NS]	0.625±0.035 [NS]	0.855±0.005[b]	0.82±0.01[b]	0.88±0.01[a]
b*	0.855±0.005 [a]	0.825±0.015[b]	0.835±0.035[b]	1.685±0.045[a]	1.475±0.005 [b]	1.495±0.015[b]
hue angle (h*)	1.574±0.012 [NS]	1.818±0.033 [NS]	1.605±0.089 [NS]	1.227±0.0075 [a]	1.229±0.01[b]	1.136±0.012[c]
Whitening index (WI)	45.99±0.02 [NS]	46.02±0.015 [NS]	46.314±0.174 [NS]	47.491±0.016 [a]	47.282±0.01 [b]	47.366±0.014[b]
Yellow Index (YI)	2.654±0.016 [a]	2.56±0.047[b]	2.574±0.098[b]	5.065±0.136[a]	4.453±0.015 [b]	4.512±0.043[b]

Browning Index (BI)	2.826±0.019 [a]	2.627±0.048[b]	2.748±0.048[b]	4.763±0.089[a]	4.343±0.01[b]	4.469±0.0015
Color change ΔE	0.11±0.01[c]	0.17±0.01[b]	0.29±0.014[a]	2.525±0.05[a]	2.255±0.015 [b]	2.335±0.025[b]

400 Means with different superscripts in the same row represent significant (p < 0.05) differences

401 from each other.

3.5 Fourier transmission infrared spectrum of millet flour

403 The FTIR spectra of control and NECP-treated PMF and SMF samples are shown in Fig. 4.

404 The FTIR spectra depicted the C-H stretching vibration, the starch functional groups (O-H),

405 and the glucose pyranose vibrational twisting patterns in specific locations, namely 2800-3000

406 cm^{-1}, 3000-3600 cm^{-1}, and 800-1200 cm^{-1}. The range of 1600–1700 cm^{-1} is used to indicate the

407 stretching of the C O bond, while the range of 1500–1600 cm^{-1} is used to indicate the vibration

408 of the N H bond. The difference in absorbance observed between the PMF and SMF samples

409 could indicate a change in functional group concentration due to complexity in their structure.

410 All treated and control samples had a similar absorbance pattern, indicating that no new

411 functional groups had formed in the sample; however, there was a difference in the intensity

412 of NECP-treated samples due to the interaction with free radicals generated during the course

413 of cold plasma(14). The FTIR spectra of PMF and SMF subjected to treatments of 5 and 10

414 minutes displayed clearly identifiable peaks, as depicted in the Figure. The sample exhibited a

415 prominent peak at a wavenumber of 3391 cm^{-1}. This peak elongated in the treated samples,

416 which is associated with the elongation of OH bonds. The glycosidic bonds of the starch

417 molecules are being attacked by reactive oxygen and nitrogen species (RONS), which provide

418 powerful intermolecular interactions via RONS found in the cold plasma (45). The breakdown

419 of starch components is caused by these bonds, which demonstrate C-H stretching at 2926 and

420 2849 cm^{-1}. The analysis revealed further peaks at 1746, 1547, 1650, 1162, and 1012 cm^{-1},

421 corresponding to the primary amide, secondary amide of C–O stretching, C–C stretching, and

422 alkene group of C–C bending, respectively. Zhou et al. (2018) (46) reported the presence of

423 absorption peaks at 1167 cm^{-1}, 1079 cm^{-1}, and 994 cm^{-1}. Similarly, Chaple et al. (2020)

424 (28) found analogous peaks in the region of 1600–1700 cm^{-1}. These data suggest that the

425 starch granules underwent oxidation as a result of the influence of plasma species (10,12). In

426   addition, the transmittance in the 800–1200 cm-1 band for the sample shows an increase

427   compared to the control, indicating alterations in the crystallinity of starch granules and the

428   promotion of more organized C-O-C arrangements. The carbonyl groups (C=O) are produced

429   through the oxidation of hydroxyl (OH) groups in starch by reactive oxygen species (ROS)
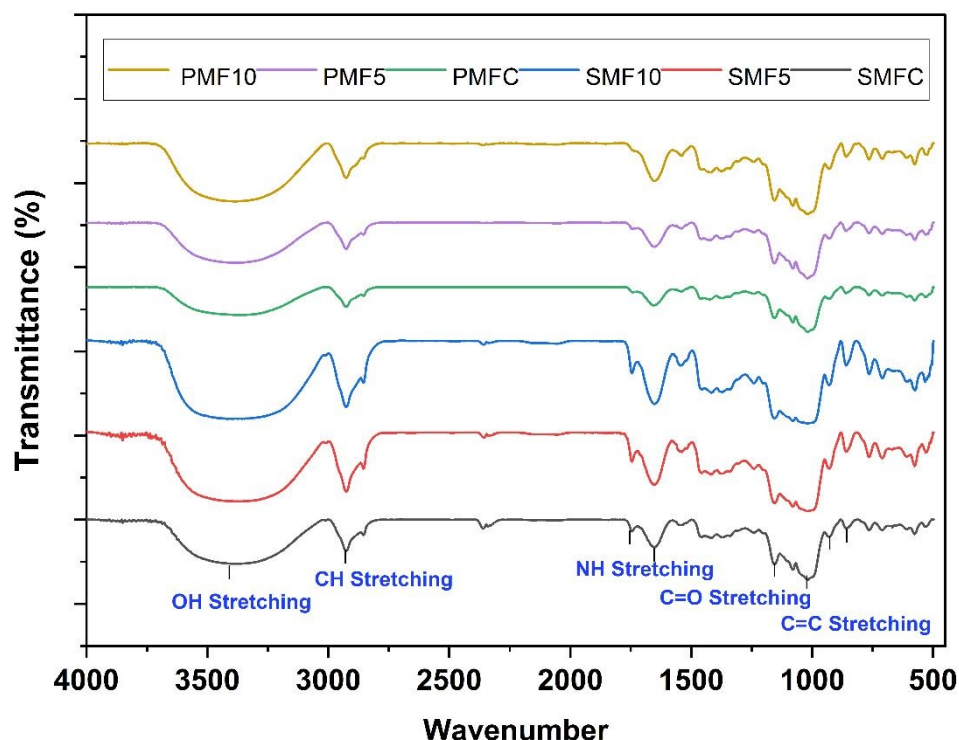
430   created during cold plasma treatment (23).

431

432

433   Fig. 4 FTIR spectra of PMF and SMF treated with NECP

434

435   **3.6 Thermographs of millet flour**

436   Table 3 summarizes the thermal properties of both the control and NECP-treated samples,

437   which include the onset temperature (To), peak temperature (Tp), and conclusion temperature

438   (Tc). Thermographs of treated and control PMF and SMF are shown in Fig. 5. The changes in

439   the physical state and crystalline structure of flour can be caused by either absorbing heat

440   (endothermic) or releasing heat (exothermic). The gelatinization temperatures of samples

441   treated with PMF and SMF were somewhat lower in comparison to the untreated samples. The

442   NECP-treated samples exhibited an earlier onset temperature (To) compared to the untreated

443   ones. This can be due to a higher level of damage caused by plasma species to the molecular

444 structure of starch. The peak temperature (Tp) of the PMFC was 101.8 °C. In the PMF5 sample,

445 the peak temperature decreased to 98.85 °C, while in the PMF10 sample, it decreased further

446 to 93.53 °C. Similarly, the peak temperature (Tp) of the SMF5 and SMF10 decreased to 86.53

447 and 76.37 °C, respectively, compared to the SMFC, which had a temperature of 87.79 °C.

448 Thirumdas et al. (2017) (47) reported a comparable reduction in the gelatinization temperature

449 of rice starch following cold plasma treatment. This endothermic shift is associated with the

450 depolymerization or alteration in the ratio of amylose and amylopectin in starch granules and

451 complete degradation of the starch crystalline structure by NECP-generated species (48).

452 Similarly, the peak temperatures were decreased for little millet flour treated with multipin cold

453 plasma employing varying power and treatment time (20). However, Sarkar et al. (2023) (49)

454 reported that the pearl millet flour samples subjected to cold plasma exhibited a slightly

455 elevated peak temperature (Tp), which could be attributed to the formation of cross-links

456 induced by plasma species. Wongsagonsup et al. (2014) (50) previously documented that the

457 lower plasma power levels cause the plasma species to start the process of connecting starch

458 chains, whereas greater plasma power levels result in the breakdown of starch chains. In our

459 earlier research, we observed that the peak gelatinization temperature increases while using

460 low-power plasma. Therefore, in this investigation, we treated all the samples by applying a

461 higher voltage of approximately 9 kV. The gelatinization enthalpy (ΔH) decreases slightly from

462 194.93 J/g to 153.85 J/g in PMF5 and 150.72 J/g in PMF10. Similarly, gelatinization enthalpy

463 (ΔH) is reduced to 151.53 J/g and 140.37 J/g in SMF5 and SMF10, as compared to untreated

464 SMF, which had a gelatinization enthalpy of 182.76 J/g. The PMF 10 and SMF10 resulted in

465 a significant reduction in the gelatinization enthalpy, with a maximum decrease of 22.67% and

466 23.17% respectively. The reduction in enthalpy indicates that the millet flour treated with non-

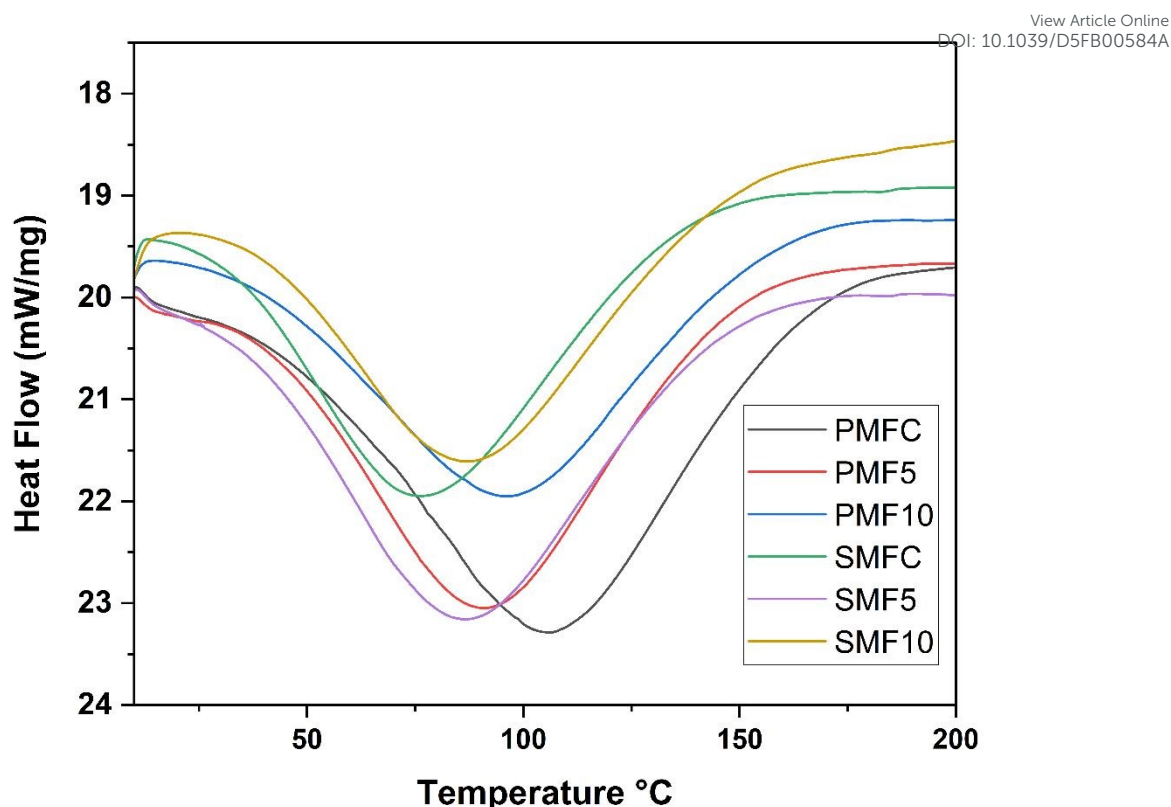467 equilibrium cold plasma requires less energy for gelatinization.

Fig. 5 Thermograph of untreated and NECP-treated PMF and SMF

3.7. Effect of NECP on structural properties of millet flour

The Fig.6 illustrates the XRD spectrum used to examine the effect of NECP treatment on the crystal structure of PMF and SMF. The spectra clearly demonstrate the presence of semicrystalline areas in both the PMF and SMF, characterized by a closely packed and organized arrangement of starch molecules. The X-ray diffraction (XRD) patterns of the millet flour samples exhibited wide peaks, suggesting the presence of a type-A crystalline pattern, which is evident from the prominent peaks at 2θ values of 15.14˚, 17.12˚, 17.94˚, 20.04˚, 22.94˚, and 26.52˚. Furthermore, there are dispersed peaks that signify the existence of non-crystalline areas. The crystallinity percentage in PMF increases with NECP treatment, which was 26.48% in PMFC and increased to 29.34% and 31.4% in PMF5 and PMF10, respectively (Table 3). Similarly, the level of crystallinity in the SMF5 (27.18%) and SMF10 (28.63%) was higher than that of the SMFC (25.38%). The increase in crystallinity is attributed to the deterioration of non-crystalline portions of starch molecules caused by NECP treatments. The NECP treatment may have caused alterations in starch granules, such as breakdown and

484 depolymerization, due to interactions with RONS. Moreover, reactive plasma species clash

485 with starch constituents such as amylose and amylopectin, resulting in an increase in the

486 number of sites accessible for starch-water interaction and, consequently, an increase in the

487 water solubility index (51). Kaur & Annapure (2024) (52) reported that the impact of

488 atmospheric cold plasma on finger millet resulted in an increase in relative crystallinity and

489 subsequently led to an increase in the water solubility index. Therefore, NECP-treated samples

490 led to the creation of starches that exhibited greater stability and solubility in comparison to

491 the control.

492 Table 3. Effect of NECP on Thermal properties and crystallinity of pearl millet and sorghum

493 millet flour

494

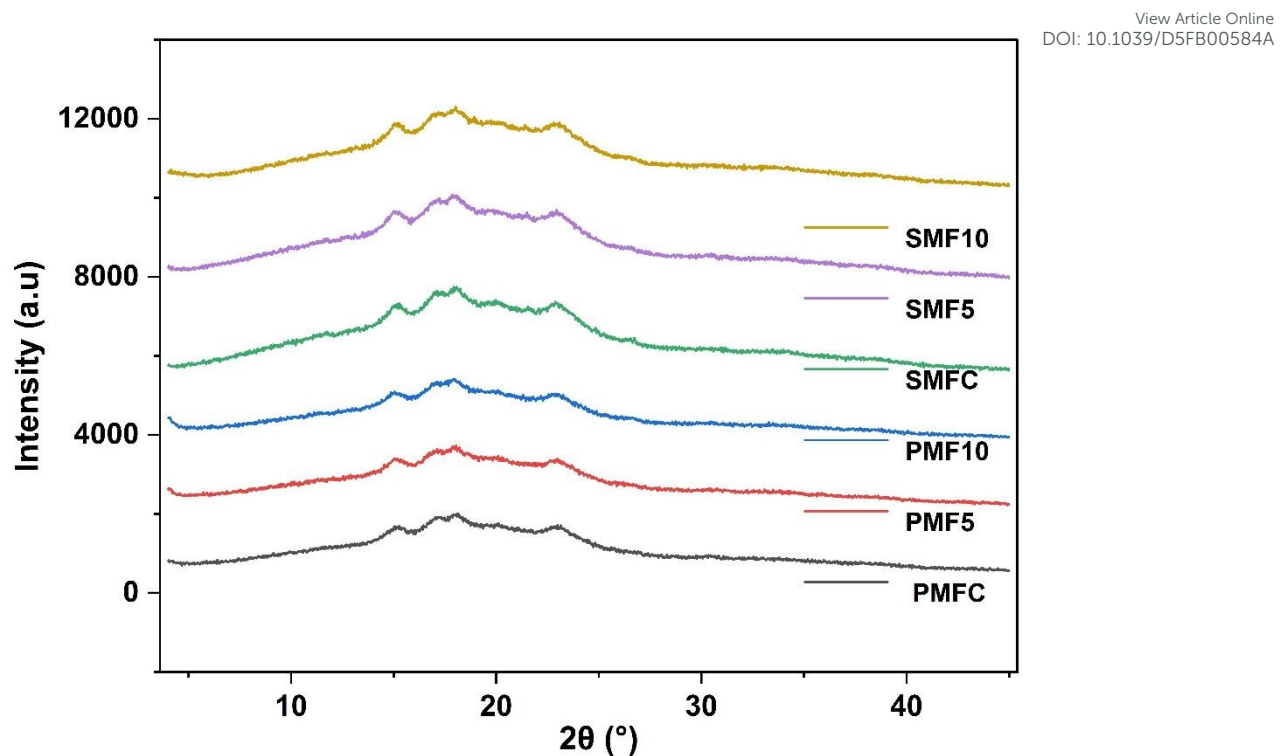|	To	Tp	Tc	ΔH	Degree of gelatinization	% Crystallinity
	℃	℃	℃	J/g	%	%
PMFC	32.23	101.8	175.25	194.93	NA	26.48
PMF5	31.23	98.85	168.25	153.85	21.07%	29.34
PMF10	29.56	93.53	166.92	150.72	22.07%	31.4
SMFC	38.56	87.79	150.07	182.76	NA	25.38
SMF5	36.73	86.53	157.06	151.53	17.08%	27.187
SMF10	34.4	76.37	162.23	140.37	23.15%	28.635

495

496

497 Fig. 6 Diffractograms of untreated and NECP-treated PMF and SMF

3.8 Effect of NECP on antinutritional factors

499 The effect of NECP treatment on antinutritional factors in PMF and SMF is illustrated in Fig.
500 7, showing a progressive and significant reduction in both tannin and phytic acid content with
501 increasing treatment time (0, 5, and 10 minutes). In PMF, the tannin content decreased from
502 approximately 250 mg/100 g to 145 mg/100 g, and phytic acid content reduced from 545
503 mg/100 g to 395 mg/100 g. Similarly, in SMF, tannin content declined from 232 mg/100 g to
504 143 mg/100 g, while phytic acid content decreased from 511 mg/100 g to 368 mg/100 g. These
505 results indicate a dose-dependent degradation of antinutritional compounds, attributed to the
506 action of plasma-generated RONS such as hydroxyl radicals ($\bullet$OH), ozone (O_3), nitric oxide
507 (NO), and peroxynitrite ($ONOO^-$), which are known to induce oxidative cleavage of phenolic
508 and phosphate-rich compounds (53). Similar observations were reported by Kheto et al. (2023)
509 (41), where atmospheric pressure cold plasma treatment significantly reduced phytic acid and
510 improved protein digestibility in guar seed flour. Likewise, R L et al. (2021) (16) demonstrated
511 that cold plasma exposure decreased phytic acid content in pearl millet by up to 60.66%,
512 attributing the effect to oxidative breakdown of phytate rings and possible activation of
513 endogenous phytase enzymes. In another study, Pankaj et al. (2018) (54) emphasized the ability
514 of plasma to disrupt antinutritional factors in legumes and cereals without compromising the

21

515 structural integrity of starch and protein fractions. The parallel downward trends of tannins and

516 phytic acid in the current study suggest that both compounds are similarly susceptible to

517 oxidative degradation, supporting the hypothesis that cold plasma can act as a non-thermal,

518 residue-free processing tool for improving the nutritional and functional properties of millet

519 flours. The minimal variability observed in replicates (indicated by small error bars) confirms

520 the reproducibility and consistency of the treatment. These findings validate NECP as a

521 sustainable and scalable intervention for enhancing millet flour quality, especially for

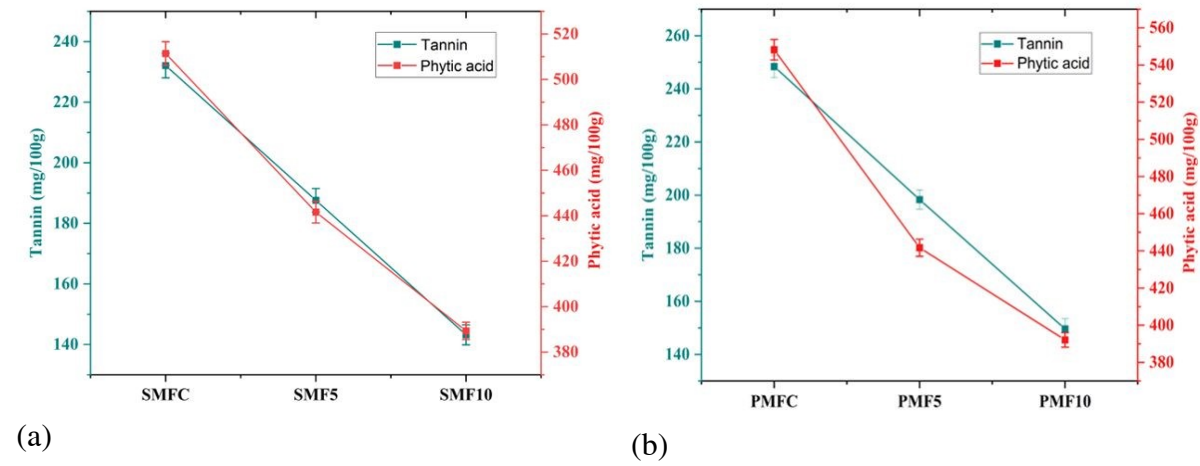522 applications in functional food formulations where digestibility and mineral bioavailability are

523 critical.

524

(a)　　　　　　　　　　　　　　　　　　　　(b)

525   Fig. 7 Tannin and phytic acid in untreated and NECP-treated (a) SMF and (b) PMF

526

527 **3.9 Principal component analysis**

528 The study examined the correlations between the functional, bioactive chemicals, color, and

529 thermal properties using Principal Component Analysis (PCA). The results revealed two

530 principal components, PC1 (57.33%) and PC2 (37.09%), which accounted for a total of 94.42%

531 of the overall variation (Fig. 8). None of the variables are directly related to any PCs. The

532 untreated samples of SMFC and PMFC were located in the lower left and right quadrants,

533 respectively, indicating disparities in the characteristics of the SMF and PMF samples. While

534 NECP treated SMF10, SMF5, and PMF10, the samples were positioned in the upper left and

535 right quadrants, which suggests notable variations in characteristics compared to the untreated

536 samples. This suggests that a prolonged period of plasma treatment, specifically 10 minutes, is

537   required for the plasma-generated reactive oxygen and nitrogen species (RONS) to sufficiently

538   engage with the flour and influence the functionality of the treated samples.

539   While these results highlight the promise of NECP as an emerging alternative to conventional

540   thermal processing, still there are certain challenges. The generation and distribution of reactive

541   species can fluctuate depending on humidity, gas composition, and processing distance and

542   may affect reproducibility. Potential oxidative changes to lipids or sensitive bioactive

543   components may also occur under prolonged exposure, which raises questions regarding long-

544   term storage stability. Lack of established treatment protocols, limited continuous-processing

545   designs, and the requirement for energy-efficiency evaluation are additional obstacles to

546   industrial-scale implementation. Therefore, although NECP demonstrates strong potential for

547   quality enhancement of millet flours, further research is required to address these constraints,

548   particularly by investigating long-term shelf stability, optimizing process uniformity, and

549   validating its technological applicability across diverse food matrices. In addition, further study

550   is required to confirm the suitability of the NECP treatment to improve the functionality of the
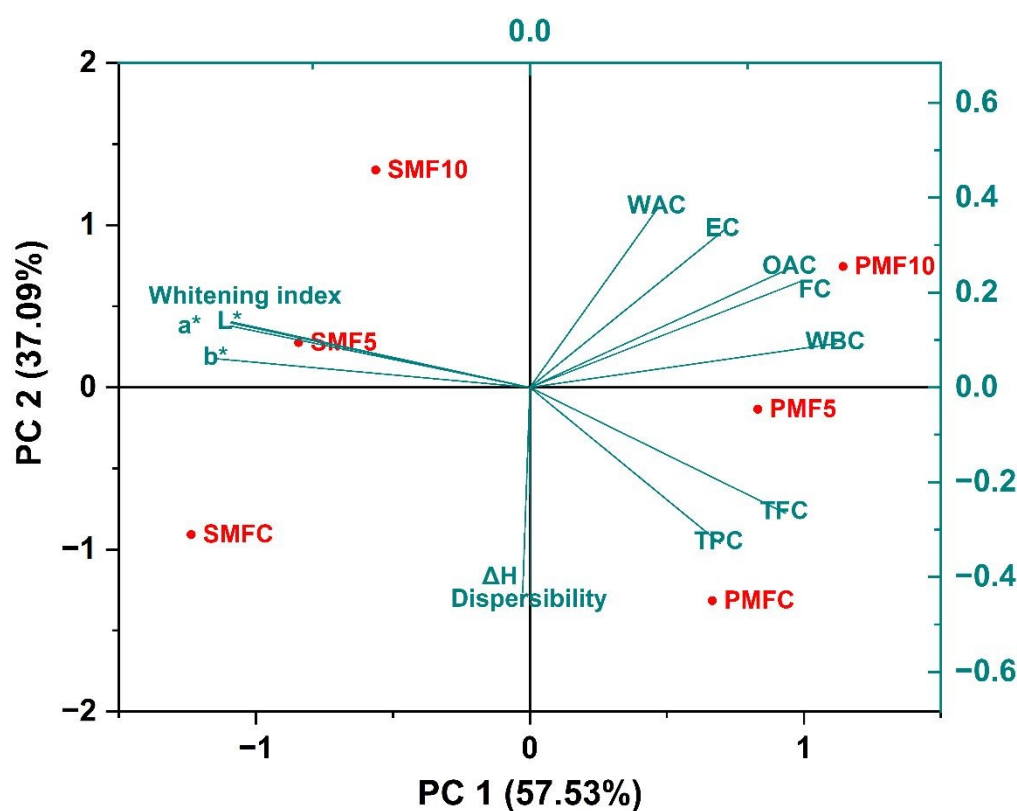
551   millet flour.

553   Fig. 8 Biplot of PCA analysis of NECP-treated pearl sorghum millet flour.

554   **3.10 Effect on Microstructural Changes**

555 The microstructural changes induced by NECP treatment in PMF and SMF were examined

556 using FESEM and are shown in Fig. 9. The control samples exhibited compact, well-defined

557 starch granules with smooth, intact surfaces, reflecting minimal structural disturbance. In

558 contrast, the NECP-treated samples showed noticeable morphological alterations, with the

559 degree of surface disruption increasing progressively with treatment duration. For the 5-minute

560 NECP treatment (PMF5 and SMF5), the granules began to show subtle surface roughening,

561 shallow pits, and minor fissures. These features suggest the initial stages of etching is caused

562 by plasma-generated reactive species. The interaction of ions, radicals, and excited molecules

563 with the granule surface likely resulted in partial removal of the outer layers and weakening of

564 amorphous regions. The effect was more pronounced in the 10-minute treated samples (PMF10

565 and SMF10), where the granules displayed significant erosion, deeper cracks, and hollowed

566 regions. Such extensive disruption indicates increased penetration of plasma ions into the

567 granular matrix, leading to degradation of amorphous domains and destabilization of the

568 surface architecture. The stronger etching at longer exposure times is consistent with intensified

569 interaction of RONS with starch and protein components.

570 The FESEM observations are well supported by the structural and thermal transitions reflected

571 in the XRD and DSC analyses. The progressive surface erosion, fissures, and granular

572 disruption seen in NECP-treated PMF and SMF correspond with the increase in relative

573 crystallinity observed in the XRD patterns. The breakdown of amorphous regions by plasma-

574 generated reactive species likely facilitated the reorganization of remaining starch chains into

575 more ordered crystalline domains, as reflected by the higher crystallinity values in PMF10 and

576 SMF10. This structural rearrangement also aligns with the decrease in gelatinization enthalpy

577 (ΔH) and the shift toward lower onset and peak gelatinization temperatures in the DSC

578 thermograms. These findings are consistent with earlier studies reporting that cold plasma

579 exposure causes surface etching, deformation of granules, and the development of cavities in

580 starch and protein-based systems (55–58). The microstructural breakdown observed in PMF10

581 and SMF10 supports the enhanced functional and thermal properties discussed earlier, as

582 plasma-induced surface roughness and fissures increase the accessibility of hydrophilic and

583 hydrophobic sites, thereby influencing absorption, gelatinization, and solubility behaviour
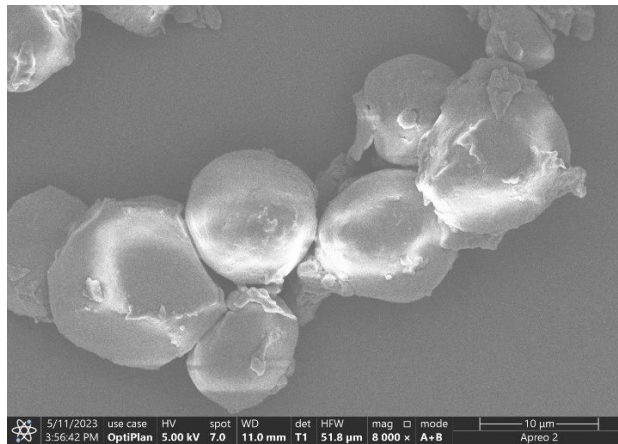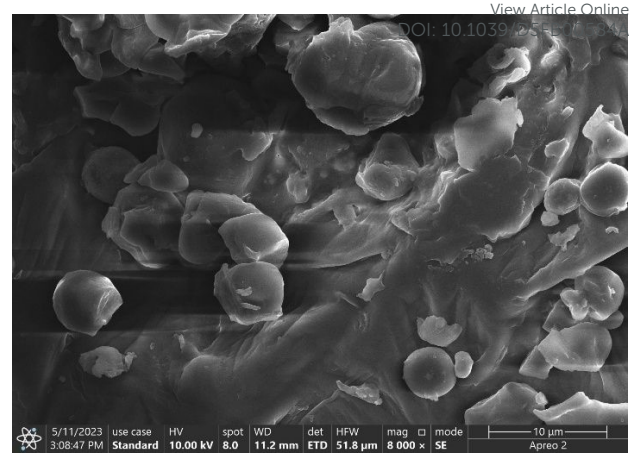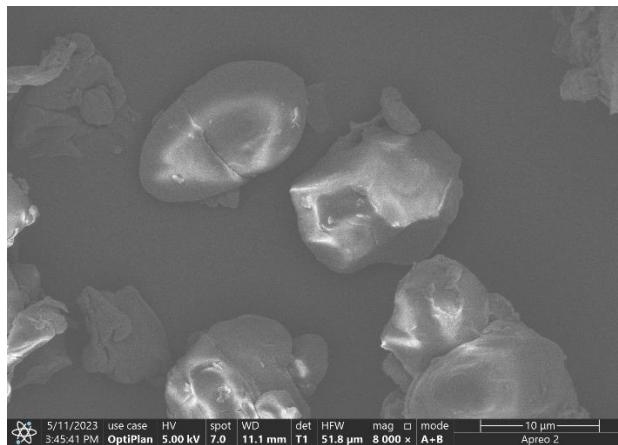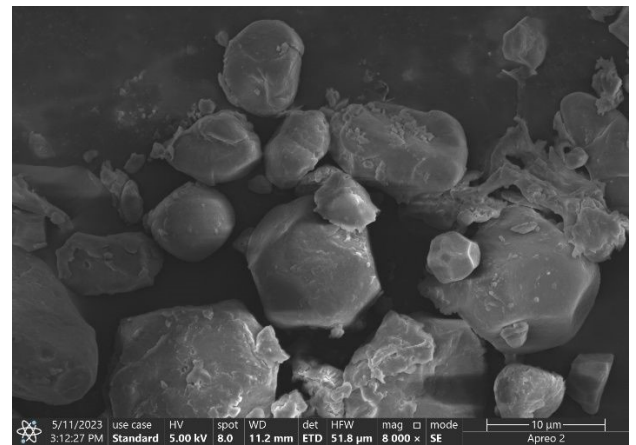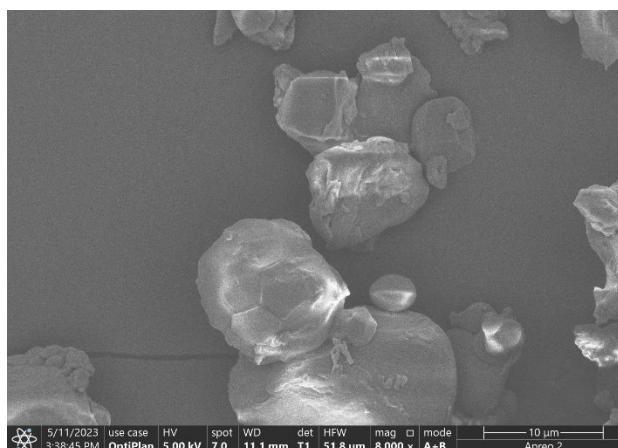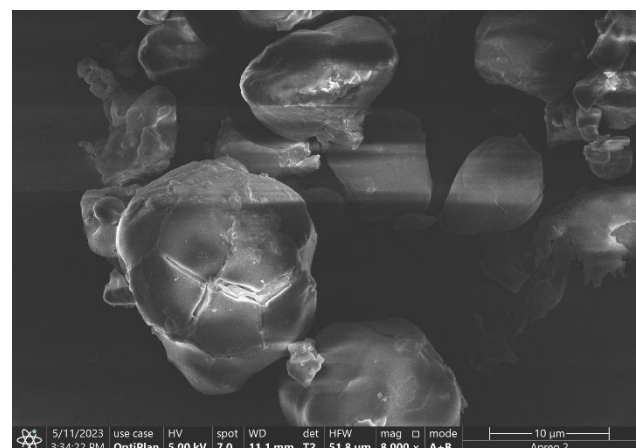
584 (59).

PMF C

SMF C

PMF 5

SMF 5

PMF 10

SMF 10

585   Fig. 9 FESEM images of NECP-treated PMF and SMF

586

4. Conclusions

587

588 This study illustrates the efficiency of non-equilibrium cold plasma treatment using a DBD
589 source made of a stator and a rotator electrode arrangement. These features enable easy
590 scalability and enhance commercial viability without requiring significant redesign. The
591 application of NECP treatment to pearl and sorghum millet flour resulted in notable changes
592 to its functional and physical properties. Specifically, the treatment led to a decrease in
593 dispersibility, alongside increases in oil holding capacity, water holding capacity, and water
594 binding capacity. Importantly, no color changes were observed post-treatment. The increase in
595 peak gelatinization temperature is attributed to the depolymerization of starch molecules
596 induced by the plasma treatment. Overall, the enhanced functional properties of pearl and
597 sorghum millet flour post-NECP treatment suggest its potential as a potent component for novel
598 food formulations, such as breads, porridges, and frozen goods. NECP emerges as a promising
599 alternative to traditional heat processing methods, offering a means to improve the quality of
600 millet flour without compromising its physical properties. These findings highlight the
601 potential of NECP to alter the physical and functional characteristics of millet flour, making it
602 a potent component for the food industry.

603 However, further research is necessary to validate the suitability of plasma-treated millet flour
604 for broader applications within the food industry.

Author contributions

605

606 Ritesh Mishra - wrote the original draft, contributed to review and editing, and was responsible
607 for visualization, software, methodology, investigation, formal analysis, data curation, and
608 conceptualization. Sushma Jangra - methodology, formal analysis, and investigation. Abhijit
609 Mishra – methodology, investigation, and data curation. Shikha Pandey – methodology and
610 data curation. Meenu Chhabra - review and editing, conceptualization, and supervision. Ram
611 Prakash - review and editing, visualization, conceptualization, and supervision.

Conflicts of interest

612

613 The authors declare that they have no conflict of interest.

Data availability

614

615 All the data is presented within the manuscript itself.

Acknowledgements

616

619   **References**

620   1.   Panwar P, Dubey A, Verma AK. Evaluation of nutraceutical and antinutritional
621   properties in barnyard and finger millet varieties grown in Himalayan region. J Food
622   Sci Technol. 2016 Jun 20;53(6):2779–87.

623   2.   Falguera V, Aliguer N, Falguera M. An integrated approach to current trends in food
624   consumption: Moving toward functional and organic products? Food Control. 2012
625   Aug;26(2):274–81.

626   3.   Conte P. Technological and Nutritional Challenges, and Novelty in Gluten-Free
627   Breadmaking: a Review. Pol J Food Nutr Sci. 2019 Mar 1;69(1):5–21.

628   4.   Joshi TJ, Singh SM, Rao PS. Novel thermal and non-thermal millet processing
629   technologies: advances and research trends. European Food Research and Technology.
630   2023 May 7;249(5):1149–60.

631   5.   Yousaf L, Hou D, Liaqat H, Shen Q. Millet: A review of its nutritional and functional
632   changes during processing. Food Research International. 2021 Apr;142:110197.

633   6.   Mishra R, Chhabra M, Prakash R. Non-equilibrium cold plasmas and their impacts on
634   physico-chemical properties of food items. Rev Mod Plasma Phys. 2025 Apr
635   25;9(1):16.

636   7.   Jangra S, Mishra R, Mishra A, Pandey S, Prakash R. Analysis of short-term treatment
637   effects of dielectric barrier discharge plasma to improve germination characteristics of
638   wheat seeds. Radiation Effects and Defects in Solids. 2024 Jul 3;179(7–8):1023–31.

639   8.   Mishra R, Pandey S, Jangra S, Mishra A, Chhabra M, Prakash R. Effective microbial
640   control, enhancing antioxidant activity and pesticide removal in fresh cut apples with
641   plasma activated water. Postharvest Biol Technol. 2025 Oct;228:113660.

642   9.   Pandey S, Jangra R, Ahlawat K, Mishra R, Mishra A, Jangra S, et al. Selective
643   generation of nitrate and nitrite in plasma activated water and its physicochemical
644   parameters analysis. Physics Letters, Section A: General, Atomic and Solid State
645   Physics [Internet]. 2023;474:128832. Available from:
646   https://doi.org/10.1016/j.physleta.2023.128832

647   10. Misra NN, Kaur S, Tiwari BK, Kaur A, Singh N, Cullen PJ. Atmospheric pressure
648   cold plasma (ACP) treatment of wheat flour. Food Hydrocoll. 2015 Feb;44:115–21.

649   11. Jangra S, Mishra R, Mishra A, Pandey S, Prakash R. Enhancing Physicochemical and
650   Functional Properties of Wheat Flour by Dielectric Barrier Discharge Plasma
651   Treatment. ACS Food Science & Technology. 2025 Mar 13;

652   12. Jaddu S, Pradhan RC, Dwivedi M. Effect of multipin atmospheric cold plasma
653   discharge on functional properties of little millet (Panicum miliare) flour. Innovative
654   Food Science & Emerging Technologies. 2022 May;77:102957.

655   13. K Joy J, Kalaivendan RGT, Eazhumalai G, Kahar SP, Annapure US. Effect of pin-to-
656   plate atmospheric cold plasma on jackfruit seed flour functionality modification.
657   Innovative Food Science & Emerging Technologies. 2022 Jun;78:103009.

658   14.   Zare L, Mollakhalili-Meybodi N, Fallahzadeh H, Arab M. Effect of atmospheric
659   pressure cold plasma (ACP) treatment on the technological characteristics of quinoa
660   flour. LWT. 2022 Feb;155:112898.

661   15.   Mishra R, Jangra S, Mishra A, Pandey S, Prakash R, Chhabra M. Enhancement of
662   structural and functional characteristics of millet flours using non-equilibrium cold
663   plasma. Radiation Effects and Defects in Solids. 2024 Jul 3;179(7–8):881–7.

664   16.   R L, P. S S, R M. Improvement in Millet Soaking by Way of Bubbled Cold Plasma
665   Processed Air Exposure; Phytic Acid Reduction Cum Nutrient Analysis Concern.
666   Frontiers in Advanced Materials Research. 2021 Oct 30;1–16.

667   17.   Sun X, Saleh ASM, Lu Y, Sun Z, Zhang X, Ge X, et al. Effects of ultra-high pressure
668   combined with cold plasma on structural, physicochemical, and digestive properties of
669   proso millet starch. Int J Biol Macromol. 2022 Jul;212:146–54.

670   18.   Rao M, Akhil K, … CSIntJC, 2021 undefined. Effect of microwave treatment on
671   physical and functional properties of foxtail millet flour. researchgate.net [Internet].
672   2021 Jan 1 [cited 2023 May 5];9(1):2762–7. Available from:
673   https://www.researchgate.net/profile/Sunil-C-
674   K/publication/349237467_Effect_of_microwave_treatment_on_physical_and_function
675   al_properties_of_foxtail_millet_flour/links/60261ccb299bf1cc26bce9c8/Effect-of-
676   microwave-treatment-on-physical-and-functional-properties-of-foxtail-millet-flour.pdf

677   19.   Jaddu S, Abdullah S, Dwivedi M, Pradhan RC. Multipin cold plasma electric discharge
678   on hydration properties of kodo millet flour: Modelling and optimization using
679   response surface methodology and artificial neural network – Genetic algorithm. Food
680   Chemistry: Molecular Sciences. 2022 Dec;5:100132.

681   20.   Jaddu S, Pradhan RC, Dwivedi M. Effect of multipin atmospheric cold plasma
682   discharge on functional properties of little millet (Panicum miliare) flour. Innovative
683   Food Science & Emerging Technologies. 2022 May;77:102957.

684   21.   Sarkar A, Niranjan T, Patel G, Kheto A, Tiwari BK, Dwivedi M. Impact of cold
685   plasma treatment on nutritional, antinutritional, functional, thermal, rheological, and
686   structural properties of pearl millet flour. J Food Process Eng. 2023 May 15;46(5).

687   22.   Sarkar A, Niranjan T, Patel G, Kheto A, Tiwari BK, Dwivedi M. Impact of cold
688   plasma treatment on nutritional, antinutritional, functional, thermal, rheological, and
689   structural properties of pearl millet flour. J Food Process Eng. 2023 May 15;46(5).

690   23.   Sharma V, Tomar MS, Sahoo S, Pradhan RC. Development of barnyard millet flour
691   rich in bioactive compounds with enhanced functional properties by application of
692   multipin atmospheric cold plasma. J Food Process Eng. 2024 Jun 20;47(6).

693   24.   Jangra S, Mishra A, Mishra R, Pandey S, Prakash R. Transformative impact of
694   atmospheric cold plasma on mung bean seeds: Unveiling surface characteristics,
695   physicochemical alterations, and enhanced germination potential. AIP Adv. 2024 Jul
696   1;14(7).

697   25.   Mishra A, Mishra R, Siddiqui YH, Jangra S, Pandey S, Prakash R. Analysis of
698   discharge parameters of an Argon Cold Atmospheric Pressure Plasma Jet and its
699   impact on surface characteristics of White Grapes. Phys Scr. 2024 Sep 16;

700   26.   Attri P, Ishikawa K, Okumura T, Koga K, Shiratani M. Plasma Agriculture from
701   Laboratory to Farm: A Review. Processes. 2020 Aug 17;8(8):1002.

702 27. Pandey S, Mishra R, Mishra A, Jangra S, Prakash R. Plasma Activated Water
703   Generation in Pin-to-Plate Gas Phase DBD-based Plasma Source for Enhanced
704   Biochemical Activity. Phys Lett A. 2025 Jan;130245.
705 28. Chaple S, Sarangapani C, Jones J, Carey E, Causeret L, Genson A, et al. Effect of
706   atmospheric cold plasma on the functional properties of whole wheat (Triticum
707   aestivum L.) grain and wheat flour. Innovative Food Science & Emerging
708   Technologies. 2020 Dec;66:102529.
709 29. Mishra R, Mishra A, Jangra S, Pandey S, Chhabra M, Prakash R. Process parameters
710   optimization for red globe grapes to enhance shelf-life using non-equilibrium cold
711   plasma jet. Postharvest Biol Technol. 2024 Apr;210:112778.
712 30. Mishra A, Jangra S, Mishra R, Pandey S, Soundharrajan P, Kombade SP, et al.
713   Characterization Study of a Helium Cold Atmospheric-Pressure Plasma Jet and Its
714   Application in Plasma-Mediated Root Canal Irrigation. IEEE Trans Radiat Plasma
715   Med Sci. 2025;1–1.
716 31. Quinton L. American Association of Cereal Chemists Approved Methods, 10th ed.,
717   CD-ROM American Association of Cereal Chemists, 2000, ISBN: 1-891127-13-6,
718   US$579. Carbohydr Polym. 2002 Sep 1;49(4):515.
719 32. Kheto A, Joseph D, Islam M, Dhua S, Das R, Kumar Y, et al. Microwave roasting
720   induced structural, morphological, antioxidant, and functional attributes of Quinoa (
721   Chenopodium quinoa Willd). J Food Process Preserv. 2022 May 8;46(5).
722 33. Kulkarni KD, Kulkarni DN, Ingle UM. Sorghum Malt-Based Weaning Food
723   Formulations: Preparation, Functional Properties, and Nutritive Value. Food Nutr Bull.
724   1991 Dec 1;13(4):1–7.
725 34. Pathare PB, Opara UL, Al-Said FAJ. Colour Measurement and Analysis in Fresh and
726   Processed Foods: A Review. Food Bioproc Tech. 2013 Jan 11;6(1):36–60.
727 35. Ali HM, El-Gizawy AM, El-Bassiouny REI, Saleh MA. The role of various amino
728   acids in enzymatic browning process in potato tubers, and identifying the browning
729   products. Food Chem. 2016 Feb;192:879–85.
730 36. Yadav S, Mishra S, Pradhan RC. Ultrasound-assisted hydration of finger millet
731   (Eleusine Coracana) and its effects on starch isolates and antinutrients. Ultrason
732   Sonochem. 2021 May;73:105542.
733 37. Mishra A, P. S, Kumar P, Prakash R. Comparative analysis of disinfection
734   effectiveness of Helium CAP jet, sodium hypochlorite and QMix in Enterococcus
735   faecalis infected root canals. Radiation Effects and Defects in Solids. 2024 Jul
736   3;179(7–8):1009–16.
737 38. Damodaran S, Paraf A. Food Proteins and their Applications. CRC Press; 2017.
738 39. Sarangapani C, Thirumdas R, Devi Y, Trimukhe A, Deshmukh RR, Annapure US.
739   Effect of low-pressure plasma on physico–chemical and functional properties of
740   parboiled rice flour. LWT - Food Science and Technology. 2016 Jun;69:482–9.
741 40. Iwe MO, Onyeukwu U, Agiriga AN. Proximate, functional and pasting properties of
742   FARO 44 rice, African yam bean and brown cowpea seeds composite flour. Cogent
743   Food Agric. 2016 Feb 10;2(1).
744 41. Kheto A, Mallik A, Sehrawat R, Gul K, Routray W. Atmospheric cold plasma induced
745   nutritional & anti-nutritional, molecular modifications and in-vitro protein

Sustainable Food Technology Accepted Manuscript

746   digestibility of guar seed (Cyamopsis tetragonoloba L.) flour. Food Research
747   International. 2023 Jun;168:112790.

748 42. Hoque M, McDonagh C, Tiwari BK, Kerry JP, Pathania S. Effect of Cold Plasma
749   Treatment on the Packaging Properties of Biopolymer-Based Films: A Review.
750   Applied Sciences. 2022 Jan 27;12(3):1346.

751 43. Almeida FDL, Cavalcante RS, Cullen PJ, Frias JM, Bourke P, Fernandes FAN, et al.
752   Effects of atmospheric cold plasma and ozone on prebiotic orange juice. Innovative
753   Food Science & Emerging Technologies. 2015 Dec;32:127–35.

754 44. Mishra R, Mishra A, Jangra S, Pandey S, Chhabra M, Prakash R. Process parameters
755   optimization for red globe grapes to enhance shelf-life using non-equilibrium cold
756   plasma jet. Postharvest Biol Technol. 2024 Apr;210:112778.

757 45. Sarkar A, Niranjan T, Patel G, Kheto A, Tiwari BK, Dwivedi M. Impact of cold
758   plasma treatment on nutritional, antinutritional, functional, thermal, rheological, and
759   structural properties of pearl millet flour. J Food Process Eng. 2023 May 15;46(5).

760 46. Zhou Y, Yan Y, Shi M, Liu Y. Effect of an Atmospheric Pressure Plasma Jet on the
761   Structure and Physicochemical Properties of Waxy and Normal Maize Starch.
762   Polymers (Basel). 2018 Dec 21;11(1):8.

763 47. Thirumdas R, Trimukhe A, Deshmukh RR, Annapure US. Functional and rheological
764   properties of cold plasma treated rice starch. Carbohydr Polym. 2017 Feb;157:1723–
765   31.

766 48. Sumathi A, Ushakumari SR, Malleshi NG. Physico-chemical characteristics,
767   nutritional quality and shelf-life of pearl millet based extrusion cooked supplementary
768   foods. Int J Food Sci Nutr. 2007 Jan 6;58(5):350–62.

769 49. Sarkar A, Niranjan T, Patel G, Kheto A, Tiwari BK, Dwivedi M. Impact of cold
770   plasma treatment on nutritional, antinutritional, functional, thermal, rheological, and
771   structural properties of pearl millet flour. J Food Process Eng. 2023 May 15;46(5).

772 50. Wongsagonsup R, Deeyai P, Chaiwat W, Horrungsiwat S, Leejariensuk K,
773   Suphantharika M, et al. Modification of tapioca starch by non-chemical route using jet
774   atmospheric argon plasma. Carbohydr Polym. 2014 Feb;102:790–8.

775 51. da Costa Pinto C, Sanches EA, Clerici MTPS, Rodrigues S, Fernandes FAN, de Souza
776   SM, et al. Modulation of the Physicochemical Properties of Aria (Goeppertia allouia)
777   Starch by Cold Plasma: Effect of Excitation Frequency. Food Bioproc Tech. 2023 Apr
778   15;16(4):768–84.

779 52. Kaur P, Annapure US. Understanding the atmospheric cold plasma-induced
780   modification of finger millet (Eleusine coracana) starch and its related mechanisms. Int
781   J Biol Macromol. 2024 May;268:131615.

782 53. Misra NN, Yadav B, Roopesh MS, Jo C. Cold Plasma for Effective Fungal and
783   Mycotoxin Control in Foods: Mechanisms, Inactivation Effects, and Applications.
784   Compr Rev Food Sci Food Saf. 2019 Jan 18;18(1):106–20.

785 54. Pankaj SK, Wan Z, Keener KM. Effects of Cold Plasma on Food Quality: A Review.
786   Foods 2018, Vol 7, Page 4 [Internet]. 2018 Jan 1 [cited 2021 Aug 21];7(1):4. Available
787   from: https://www.mdpi.com/2304-8158/7/1/4/htm

788 55. Jaddu S, Pradhan RC, Dwivedi M. Effect of multipin atmospheric cold plasma
789   discharge on functional properties of little millet (Panicum miliare) flour. Innovative
790   Food Science & Emerging Technologies. 2022 May;77:102957.

791 56. Sarkar A, Niranjan T, Patel G, Kheto A, Tiwari BK, Dwivedi M. Impact of cold
792   plasma treatment on nutritional, antinutritional, functional, thermal, rheological, and
793   structural properties of pearl millet flour. J Food Process Eng. 2023 May 15;46(5).
794 57. Sun X, Saleh ASM, Sun Z, Ge X, Shen H, Zhang Q, et al. Modification of multi-scale
795   structure, physicochemical properties, and digestibility of rice starch via microwave
796   and cold plasma treatments. LWT. 2022 Jan;153:112483.
797 58. Gong W, Guo X lu, Huang H bo, Li X, Xu Y, Hu JN. Structural characterization of
798   modified whey protein isolates using cold plasma treatment and its applications in
799   emulsion oleogels. Food Chem. 2021 Sep;356:129703.
800 59. K Joy J, Kalaivendan RGT, Eazhumalai G, Kahar SP, Annapure US. Effect of pin-to-
801   plate atmospheric cold plasma on jackfruit seed flour functionality modification.
802   Innovative Food Science & Emerging Technologies. 2022 Jun;78:103009.

803

Sustainable Food Technology Accepted Manuscript

Data availability

All the data is presented within the manuscript itself.